EUROPEAN ORGANIZATION FOR NUCLEAR RESEARCH

CERN-EP/99-138
October 1, 1999

Search for Excited Leptons at $\sqrt{s} = 189$ GeV

The L3 Collaboration

Abstract

A search for excited leptons, e^*, μ^*, τ^*, ν_{e}^*, ν_μ^* and ν_τ^*, was performed with the L3 detector at LEP using data collected at a centre–of–mass energy of 189 GeV, corresponding to an integrated luminosity of 176 pb^{-1}. No evidence of their production is observed. From the searches for pair produced excited leptons, lower mass limits are set close to the kinematic limit. From the searches for singly produced excited leptons, upper limits on their couplings are derived in the mass range up to 189 GeV.

Submitted to *Phys. Lett. B*

1 Introduction

The existence of excited leptons would provide evidence for fermion substructure. Composite models could explain the number of families and make the fermion masses and weak mixing angles calculable [1]. The excited leptons e^*, μ^*, τ^* (collectively denoted as ℓ^*) and ν^* have been extensively searched for at the LEP e^+e^- and the HERA ep colliders [2]. These particles are assumed to have spin and isospin values 1/2 and the same electroweak SU(2) and U(1) gauge couplings to the vector bosons as the standard leptons, but are expected to constitute both left and right handed weak isodoublets. Excited leptons are expected to decay into their ground states by radiating a photon or a massive vector boson.

At e^+e^- colliders, excited leptons can be produced either in pairs ($e^+e^- \longrightarrow \ell^*\ell^*, \longrightarrow \nu^*\nu^*$) or singly ($e^+e^- \longrightarrow \ell\ell^*, \longrightarrow \nu\nu^*$). In pair production, the coupling of the excited leptons to the gauge bosons is described by the Lagrangian [3]

$$\mathcal{L}_{\ell^*\ell^*} = \bar{L}^*\gamma^\mu \left(g\frac{\vec{\tau}}{2}\vec{W}_\mu + g'\frac{Y}{2}B_\mu \right) L^*.$$

The cross section for pair production depends on the mass of the excited lepton [1,4].

Single production as well as magnetic decay can be described by means of an effective Lagrangian of the form [3]

$$\mathcal{L}_{\ell^*\ell} = \frac{gf}{\Lambda}\bar{L}^*\sigma^{\mu\nu}\frac{\vec{\tau}}{2}l_L\partial_\mu\vec{W}_\nu + \frac{g'f'}{\Lambda}\bar{L}^*\sigma^{\mu\nu}Y l_L\partial_\mu B_\nu + h.c.,$$

where Λ is the compositeness scale and f and f' are the couplings associated with the SU(2) and U(1) gauge groups of the Standard Model, respectively. They determine the production rate of single excited leptons and their branching ratio into standard leptons plus gauge bosons [4]. Table 1 shows the decay branching ratios for excited leptons for two relative values of f and f' and for different excited lepton masses.

Excited leptons are searched for in the radiative decays, $\ell^* \to \ell\gamma$, $\nu^* \to \nu\gamma$, and weak decays, $\ell^* \to \nu W$ and $\nu^* \to \ell W$. In the production of pairs of excited leptons, the search is performed considering only radiative decays or only weak decays, but not one excited lepton decaying radiatively and the other decaying weakly. Pair production searches are sensitive to excited leptons of mass up to values close to the kinematic limit, *i.e.* the beam energy. Single production searches extend the sensitivity to the mass range above the beam energy up to the centre–of–mass energy, $\sqrt{s}$.

2 Data Sample and Event Simulation

The data sample analysed corresponds to 176.4 pb^{-1} collected with the L3 detector [5] at LEP at $\sqrt{s}$ = 188.6 GeV in 1998. For the simulation of background from Standard Model processes, different Monte Carlo programs are used: Radiative Bhabha events are generated using BHWIDE [6] and TEEGG [7]. For other radiative dilepton events, $\mu\mu\gamma$, $\tau\tau\gamma$ and $\nu\nu\gamma$, the KORALZ [8] generator is used. The GGG [9] Monte Carlo is used for final states with only photons. KORALW [10] is used for the $e^+e^- \to$ WW process. PYTHIA [11] is used for $qq(\gamma)$, ZZ and Zee production and EXCALIBUR [12] is used for the $qqe\nu$ final state.

The generation of excited leptons and their decay is done according to their differential cross section [3], to optimise the selections and estimate the efficiencies. Initial state radiation is not implemented in the generation, but it is taken into account in cross section calculations. The generated events are passed through the L3 detector simulation [13], which includes the effects of energy loss, multiple scattering, interactions and decays in the detector and the beam pipe.

3 Radiative Decays

Excited leptons decaying radiatively give rise to final states with low multiplicity and high energy photons. Event selection criteria reject pure hadronic events, keeping a high signal efficiency independent of the flavour of excited leptons. This is achieved by accepting events with less than eight tracks and at least one photon with energy greater than 15 GeV in the central detector region ($|\cos\theta_\gamma| < 0.75$, where θ_γ is the photon polar angle). To reject cosmic background at least one scintillator within ± 5 ns of the beam crossing must be present. In addition, events with muons are required to have a muon track pointing to the primary vertex.

Electromagnetic clusters are identified as electrons if there is a matching track within 5° in the $r\phi$ projection. Muons are identified from tracks in the muon chambers. A minimum ionising particle in the calorimeters can be accepted as a second muon. The tau identification is based on jets constructed from calorimetric clusters, tracks and muons, with invariant mass below 3 GeV and at least one associated track. Events with charged leptons and photons in the final state are subjected to a kinematic fit which imposes energy and momentum conservation. This improves the resolution in the invariant mass of the $\ell\gamma$ pairs. These selection criteria are complemented by additional requirements specific to the production channel and the excited lepton flavour.

3.1 Pair Production

In order to select candidates for $\mathrm{e^+e^-} \longrightarrow \ell^*\ell^* \longrightarrow \ell\ell\gamma\gamma$, it is further required that two photons with energy greater than 15 GeV, at least one of them in the central region, and two lepton candidates of the same flavour must be present. The difference of the two lepton-photon masses is required to be smaller than 10 GeV and their sum greater than 100 GeV.

Event selection for $\mathrm{e^+e^-} \longrightarrow \nu^*\nu^* \longrightarrow \nu\nu\gamma\gamma$ is based on a signature with only two energetic photons in the final state. The preselection is complemented by requiring two photons in the central region with energies in the range $0.2 < E_\gamma/E_{beam} < 0.8$ and with the acoplanarity angle greater than 10°. There should be no tracks in the central tracker or in the muon chambers and the energy of calorimetric clusters other than photons must be smaller than 5 GeV.

The number of observed events, the expected background and the signal selection efficiency are reported in Table 2. The main background is due to radiative dilepton events $\mathrm{e^+e^-} \rightarrow \ell\ell\gamma\gamma, \nu\nu\gamma\gamma$.

3.2 Single production

Event selection for $\mathrm{e^+e^-} \longrightarrow \ell\ell^* \longrightarrow \ell\ell\gamma$ identifies final states with two leptons and one photon with energy greater than 20 GeV. At least one of the two possible $\ell\gamma$ invariant masses must be greater than 70 GeV. Events with just an identified electron and a photon, with invariant mass above 70 GeV, are also accepted for the excited electron selection. Thus, a high signal efficiency is kept for the signal events originating from the t-channel exchange where one electron escapes along the beam pipe.

Final states from $e^+e^- \longrightarrow \nu\nu^* \longrightarrow \nu\nu\gamma$ are characterised by a single photon with energy greater than $0.15\sqrt{s}$. Neither tracks in the tracking chamber, nor in the muon chambers should be present in the event. To reject cosmic events, no more than eight calorimetric clusters must be present, and besides the photon, none of them should exceed 5 GeV.

The number of observed events, the expected background and signal selection efficiency are reported in Table 2. The main background is due to radiative dilepton events $e^+e^- \to \ell\ell\gamma, \nu\nu\gamma$.

4 Weak Decays

Weakly decaying excited leptons, $\ell^* \to \nu W$ and $\nu^* \to \ell W$, with at least one W decaying hadronically give rise to high multiplicity final states. Selection criteria are designed to reject leptonic and two-photon events. More than three tracks and 14 calorimetric clusters are required in events with visible energy above 60 GeV.

The lepton identification is the same as for low multiplicity events except taus, which are identified as low multiplicity charged jets satisfying at least two of the following four conditions: less than four tracks associated with a jet, less than five calorimetric clusters, invariant mass smaller than 2 GeV, or at least 70% of its energy contained in a 5° half-opening cone. Final selection of the candidates requires additional criteria specific to the production channel and the excited lepton flavour.

4.1 Pair Production

Final states from $e^+e^- \to \ell^*\ell^* \to \nu\nu WW$ and $e^+e^- \to \nu^*\nu^* \to \ell\ell WW$ are similar to Standard Model WW production. Due to the large cross section, pair production of excited leptons would manifest itself as an enhancement of the measured WW cross section. A combination of four selections, denoted by qqqq, qqe, qqμ and qqτ, is used. To achieve a high signal efficiency, no attempt is made to reject the WW background.

For the qqqq selection, events with at least three charged jets and visible energy greater than 140 GeV are selected. For at least one pair of jets, their invariant mass must be in the range between 50 GeV and 110 GeV, the recoiling mass against these two jets must be greater than 50 GeV and the sum of invariant plus recoil masses must be greater than 120 GeV. To reduce the qqγ background, events with missing momentum above 30 GeV at low polar angle, $|\cos\theta_{miss}| > 0.95$, where θ_{miss} is the polar angle of the missing momentum, or an electromagnetic cluster with energy above 50 GeV are rejected.

For the qqℓ selections, events with missing momentum greater than 10 GeV, at high polar angle $|\cos\theta_{miss}| < 0.95$, and the difference between visible energy and missing momentum smaller than 165 GeV are selected. In addition an isolated lepton with energy greater than 5 GeV is required. The invariant mass of the event (without the identified lepton) must be in the range between 40 GeV and 120 GeV.

In the search for excited electron and muon neutrinos, the signal sensitivity is enhanced by requiring two additional isolated electrons or muons in the event, with energy in the range between 3 GeV and 15 GeV. Table 2 reports the yields of the selections. The background is mainly due to WW and qq(γ) production.

4.2 Single Production

Experimental signatures of $e^+e^- \rightarrow \ell\ell^* \rightarrow \ell\nu W$ and $e^+e^- \rightarrow \nu\nu^* \rightarrow \nu\ell W$ are also similar to Standard Model WW production. The hadronic decays of the W are considered, and the $qq\ell$ selections described above are applied.

They are complemented with a qq selection which requires two acoplanar hadronic jets with invariant mass in the range between 60 GeV and 100 GeV and recoil mass below 70 GeV, to cope with undetected leptons lost at low angle or releasing low energy.

Events are selected as candidates due to single excited leptons if they pass any of the $qq\ell$ or qq selections. The main backgrounds are due to WW, $qqe\nu$ and $qq(\gamma)$ production. The combined efficiency for ℓ^* and ν^* depends slightly on the mass and flavour of the excited lepton, except in the case of the excited electron, in which the efficiency increases from 9% to 47% in the e^* mass range between 95 GeV and 185 GeV, as shown in Table 2.

5 Results and Limits

Figures 1a-c show all combinations of invariant masses $m_{e\gamma}$, $m_{\mu\gamma}$ and $m_{\tau\gamma}$ above 70 GeV. Figure 1d shows the energy of the photon in the single photon selection. Figures 2a-c show the recoil mass against the identified lepton in the qqe, $qq\mu$ and $qq\tau$ selections; *i.e.* the mass of the ℓ^* candidate. Figures 2d-f show the event invariant mass for the qqe, $qq\mu$ and $qq\tau$ selections; *i.e.* the mass of the ν^* candidate. The number of observed events is consistent with the expected Standard Model background, see Table 2. For each flavour and mass of excited lepton hypothesis, the number of candidates found in data and expected from background are calculated. Taking into account the luminosity, the branching ratio (which depends on the ratio of the couplings f/f') and the efficiency, an upper limit to the signal cross section is derived. This limit is set at 95% confidence level, using Bayesian statistics and assuming a flat *a priori* distribution for the signal. In the case of pair production, the cross section only depends on the mass and charge of the excited lepton. A lower mass limit is derived from the cross section limit. In the case of single production, the cross section depends on the flavour and mass of the excited lepton and the value of the couplings f and f'. The cross section limit is then interpreted in terms of an upper limit to the coupling constant as a function of the mass of the excited lepton.

Two different scenarios are considered in order to calculate limits. In the first one, $f = f'$, the radiative decay is dominant for charged excited leptons whereas it is forbidden for excited neutrinos. In the second one, $f = -f'$, the radiative decay is forbidden for charged excited leptons whereas it is dominant for excited neutrinos. Mass limits, as well as upper limits to the coupling constant, are thus derived from radiative decays for charged excited leptons in the first case and excited neutrinos in the second case, and from weak decays in the other searches.

The results from pair production searches in both the radiative and the weak decay searches are combined to derive lower limits on the mass of excited leptons independent of the coupling constants f and f'. A scan is performed for all the possible ratios of the two couplings: $f/f' = \tan\theta$ with θ in the range 0 to π. For each value of f/f', the corresponding decay fractions $\ell^*\ell^* \rightarrow \ell\ell\gamma\gamma$ and $\ell^*\ell^* \rightarrow \nu\nu WW$ ($\nu^*\nu^* \rightarrow \nu\nu\gamma\gamma$ and $\nu^*\nu^* \rightarrow \ell\ell WW$ in the case of excited neutrinos) are calculated, and a mass limit is set. In Table 3 the lowest limit for each flavour of excited lepton is quoted.

Figure 3 shows the upper limits to the coupling constant for charged excited leptons and excited neutrinos in both scenarios. The left-hand edge of the curves indicates the lower mass limit derived from pair production searches, which is quoted in Table 3. An absolute lower mass limit of the order of 90 GeV and upper limits on the couplings in the mass range from 90 GeV to 180 GeV are set.

Acknowledgments

We wish to express our gratitude to the CERN accelerator divisions for the excellent performance of the LEP machine. We acknowledge the effort of the engineers and technicians who have participated in the construction and maintenance of the experiment.

References

[1] F. Boudjema *et al.*, "Z Physics at LEP 1", Vol.2, ed. J. Ellis *et al.*, CERN 89-08 (1989) 188 and references therein.

[2] ALEPH Coll., D. Buskulic *et al.*, Phys. Lett. **B385** (1996) 445;
DELPHI Coll., P. Abreu *et al.*, E. Phys. J. **C8** (1999) 41;
L3 Coll., M. Acciarri *et al.*, Phys. Lett. **B401** (1997) 139;
OPAL Coll., K. Ackerstaff *et al.*, Eur. Phys. J. **C1** (1998) 45;
H1 Coll., S. Aid *et al.*, Nucl. Phys. **B483** (1997) 44;
ZEUS Coll., J. Breitweg *et al.*, Z. Phys. **C76** (1997) 631.

[3] K. Hagiwara *et al.*, Z. Phys. **C29** (1985) 115.

[4] F. Boudjema *et al.*, Z. Phys. **C57** (1993) 425;
F. Boudjema *et al.*, Phys. Lett. **B240** (1990) 485;
M.B. Voloshin, *et al.*, Sov. Phys. JETP **64** (1986) 446;
M.B. Voloshin, Phys. Lett. **B209** (1988) 360.

[5] L3 Coll., B. Adeva *et al.*, Nucl. Instr. and Meth. **A289** (1990) 35;
L3 Coll., M. Chemarin *et al.*, Nucl. Instr. and Meth. **A349** (1994) 345;
L3 Coll., M. Acciarri *et al.*, Nucl. Instr. and Meth. **A351** (1994) 300;
L3 Coll., A. Adam *et al.*, Nucl. Instr. and Meth. **A383** (1996) 342.

[6] S. Jadach, *et al.*, Phys. Lett. **B390** (1997) 298.

[7] D. Karlen, Nucl. Phys. **B289** (1987) 23.

[8] S. Jadach *et al.*, Comp. Phys. Comm. **79** (1994) 503.

[9] F.A. Berends *et al.*, Nucl. Phys. **B186** (1981) 22;
CALKUL Coll., F.A. Berends *et al.*, Nucl. Phys. **B239** (1984) 395.

[10] KORALW: Version 1.21 is used. M. Skrzypek, *et al.*, Comp. Phys. Comm. **94** (1996) 216;
M. Skrzypek, *et al.*, Phys. Lett. **B372** (1996) 289.

[11] PYTHIA 5.7 and JETSET 7.4 Physics and Manual, T. Sjöstrand, CERN-TH/7112/93 (1993), revised August 1995; Comp. Phys. Comm. **82** (1994) 74.

[12] F.A. Berends, *et al.*, Nucl. Phys. **B424** (1994) 308;
F.A. Berends, *et al.*, Nucl. Phys. **B426** (1994) 344;
F.A. Berends, *et al.*, Nucl. Phys. (Proc. Suppl.) **B37** (1994) 163;
R. Kleiss *et al.*, Comp. Phys. Comm. **85** (1995) 447;
R. Pittau, Phys. Lett. **B335** (1994) 490.

[13] The L3 detector simulation is based on GEANT Version 3.15, R. Brun *et al.*, CERN DD/EE/84-1 (Revised 1987);
The GHEISHA program (H. Fesefeldt, RWTH Aachen Report PITHA 85/02 (1985)) is used to simulate hadronic interactions.

The L3 Collaboration:

M.Acciarri,[26] P.Achard,[19] O.Adriani,[16] M.Aguilar-Benitez,[25] J.Alcaraz,[25] G.Alemanni,[22] J.Allaby,[17] A.Aloisio,[28] M.G.Alviggi,[28] G.Ambrosi,[19] H.Anderhub,[47] V.P.Andreev,[6,36] T.Angelescu,[12] F.Anselmo,[9] A.Arefiev,[27] T.Azemoon,[3] T.Aziz,[10] P.Bagnaia,[35] L.Baksay,[42] A.Balandras,[4] R.C.Ball,[3] S.Banerjee,[10] Sw.Banerjee,[10] A.Barczyk,[47,45] R.Barillère,[17] L.Barone,[35] P.Bartalini,[22] M.Basile,[9] R.Battiston,[32] A.Bay,[22] F.Becattini,[16] U.Becker,[14] F.Behner,[47] L.Bellucci,[16] J.Berdugo,[25] P.Berges,[14] B.Bertucci,[32] B.L.Betev,[47] S.Bhattacharya,[10] M.Biasini,[32] A.Biland,[47] J.J.Blaising,[4] S.C.Blyth,[33] G.J.Bobbink,[2] A.Böhm,[1] L.Boldizsar,[13] B.Borgia,[35] D.Bourilkov,[47] M.Bourquin,[19] S.Braccini,[19] J.G.Branson,[38] V.Brigljevic,[47] F.Brochu,[4] A.Buffini,[16] A.Buijs,[43] J.D.Burger,[14] W.J.Burger,[32] J.Busenitz,[42] A.Button,[3] X.D.Cai,[14] M.Campanelli,[47] M.Capell,[14] G.Cara Romeo,[9] G.Carlino,[28] A.M.Cartacci,[16] J.Casaus,[25] G.Castellini,[16] F.Cavallari,[35] N.Cavallo,[28] C.Cecchi,[19] M.Cerrada,[25] F.Cesaroni,[23] M.Chamizo,[19] Y.H.Chang,[49] U.K.Chaturvedi,[18] M.Chemarin,[24] A.Chen,[49] G.Chen,[7] G.M.Chen,[7] H.F.Chen,[20] H.S.Chen,[7] X.Chereau,[4] G.Chiefari,[28] L.Cifarelli,[37] F.Cindolo,[9] C.Civinini,[16] I.Clare,[14] R.Clare,[14] G.Coignet,[4] A.P.Colijn,[2] N.Colino,[25] S.Costantini,[8] F.Cotorobai,[12] B.Cozzoni,[9] B.de la Cruz,[25] A.Csilling,[13] S.Cucciarelli,[32] T.S.Dai,[14] J.A.van Dalen,[30] R.D'Alessandro,[16] R.de Asmundis,[28] P.Déglon,[19] A.Degré,[4] K.Deiters,[45] D.della Volpe,[28] P.Denes,[34] F.DeNotaristefani,[35] A.De Salvo,[47] M.Diemoz,[35] D.van Dierendonck,[2] F.Di Lodovico,[47] C.Dionisi,[35] M.Dittmar,[47] A.Dominguez,[38] A.Doria,[28] M.T.Dova,[18,♯] D.Duchesneau,[4] D.Dufournaud,[4] P.Duinker,[2] I.Duran,[39] H.El Mamouni,[24] A.Engler,[33] F.J.Eppling,[14] F.C.Erné,[2] P.Extermann,[19] M.Fabre,[45] R.Faccini,[35] M.A.Falagan,[25] S.Falciano,[35,17] A.Favara,[17] J.Fay,[24] O.Fedin,[36] M.Felcini,[47] T.Ferguson,[33] F.Ferroni,[35] H.Fesefeldt,[1] E.Fiandrini,[32] J.H.Field,[19] F.Filthaut,[17] P.H.Fisher,[14] I.Fisk,[38] G.Forconi,[14] L.Fredj,[19] K.Freudenreich,[47] C.Furetta,[26] Yu.Galaktionov,[27,14] S.N.Ganguli,[10] P.Garcia-Abia,[5] M.Gataullin,[31] S.S.Gau,[11] S.Gentile,[35,17] N.Gheordanescu,[12] S.Giagu,[35] Z.F.Gong,[20] G.Grenier,[24] O.Grimm,[47] M.W.Gruenewald,[8] M.Guida,[37] R.van Gulik,[2] V.K.Gupta,[34] A.Gurtu,[10] L.J.Gutay,[44] D.Haas,[5] A.Hasan,[29] D.Hatzifotiadou,[9] T.Hebbeker,[8] A.Hervé,[17] P.Hidas,[13] J.Hirschfelder,[33] H.Hofer,[47] G. Holzner,[47] H.Hoorani,[33] S.R.Hou,[49] I.Iashvili,[46] B.N.Jin,[7] L.W.Jones,[3] P.de Jong,[2] I.Josa-Mutuberría,[25] R.A.Khan,[18] D.Kamrad,[46] M.Kaur,[18,◇] M.N.Kienzle-Focacci,[19] D.Kim,[35] D.H.Kim,[41] J.K.Kim,[41] S.C.Kim,[41] J.Kirkby,[17] D.Kiss,[13] W.Kittel,[30] A.Klimentov,[14,27] A.C.König,[30] A.Kopp,[46] V.Koutsenko,[14,27] M.Kräber,[47] R.W.Kraemer,[33] W.Krenz,[1] A.Kunin,[14,27] P.Ladron de Guevara,[25] I.Laktineh,[24] G.Landi,[16] K.Lassila-Perini,[47] P.Laurikainen,[21] A.Lavorato,[37] M.Lebeau,[17] A.Lebedev,[14] P.Lebrun,[24] P.Lecomte,[47] P.Lecoq,[17] P.Le Coultre,[47] H.J.Lee,[8] J.M.Le Goff,[17] R.Leiste,[46] E.Leonardi,[35] P.Levtchenko,[36] C.Li,[20] C.H.Lin,[49] W.T.Lin,[49] F.L.Linde,[2] L.Lista,[28] Z.A.Liu,[7] W.Lohmann,[46] E.Longo,[35] Y.S.Lu,[7] K.Lübelsmeyer,[1] C.Luci,[17,35] D.Luckey,[14] L.Lugnier,[24] L.Luminari,[35] W.Lustermann,[47] W.G.Ma,[20] M.Maity,[10] L.Malgeri,[17] A.Malinin,[27,17] C.Maña,[25] D.Mangeol,[30] P.Marchesini,[47] G.Marian,[15] J.P.Martin,[24] F.Marzano,[35] G.G.G.Massaro,[2] K.Mazumdar,[10] R.R.McNeil,[6] S.Mele,[17] L.Merola,[28] M.Meschini,[16] W.J.Metzger,[30] M.von der Mey,[1] A.Mihul,[12] H.Milcent,[17] G.Mirabelli,[35] J.Mnich,[17] G.B.Mohanty,[10] P.Molnar,[8] B.Monteleoni,[16,†] T.Moulik,[10] G.S.Muanza,[24] F.Muheim,[19] A.J.M.Muijs,[2] M.Musy,[35] M.Napolitano,[28] F.Nessi-Tedaldi,[47] H.Newman,[31] T.Niessen,[1] A.Nisati,[35] H.Nowak,[46] Y.D.Oh,[41] G.Organtini,[35] R.Ostonen,[21] A.Oulianov,[27] C.Palomares,[25] D.Pandoulas,[1] S.Paoletti,[35,17] P.Paolucci,[28] R.Paramatti,[35] H.K.Park,[33] I.H.Park,[41] G.Pascale,[35] G.Passaleva,[17] S.Patricelli,[28] T.Paul,[11] M.Pauluzzi,[32] C.Paus,[17] F.Pauss,[47] D.Peach,[17] M.Pedace,[35] S.Pensotti,[26] D.Perret-Gallix,[4] B.Petersen,[30] D.Piccolo,[28] F.Pierella,[9] M.Pieri,[16] P.A.Piroué,[34] E.Pistolesi,[26] V.Plyaskin,[27] M.Pohl,[47] V.Pojidaev,[27,16] H.Postema,[14] J.Pothier,[17] N.Produit,[19] D.O.Prokofiev,[44] D.Prokofiev,[36] J.Quartieri,[37] G.Rahal-Callot,[47,17] M.A.Rahaman,[10] P.Raics,[15] N.Raja,[10] R.Ramelli,[47] P.G.Rancoita,[26] G.Raven,[38] P.Razis,[29]D.Ren,[47] M.Rescigno,[35] S.Reucroft,[11] T.van Rhee,[43] S.Riemann,[46] K.Riles,[3] A.Robohm,[47] J.Rodin,[42] B.P.Roe,[3] L.Romero,[25] A.Rosca,[8] S.Rosier-Lees,[4] J.A.Rubio,[17] D.Ruschmeier,[8] H.Rykaczewski,[47] S.Saremi,[6] S.Sarkar,[35] J.Salicio,[17] E.Sanchez,[17] M.P.Sanders,[30] M.E.Sarakinos,[21] C.Schäfer,[1] V.Schegelsky,[36] S.Schmidt-Kaerst,[1] D.Schmitz,[1] H.Schopper,[48] D.J.Schotanus,[30] G.Schwering,[1] C.Sciacca,[28] D.Sciarrino,[19] A.Seganti,[9] L.Servoli,[32] S.Shevchenko,[31] N.Shivarov,[40] V.Shoutko,[27] E.Shumilov,[27] A.Shvorob,[31] T.Siedenburg,[1] D.Son,[41] B.Smith,[33] P.Spillantini,[16] M.Steuer,[14] D.P.Stickland,[34] A.Stone,[6] H.Stone,[34,†] B.Stoyanov,[40] A.Straessner,[1] K.Sudhakar,[10] G.Sultanov,[18] L.Z.Sun,[20] H.Suter,[47] J.D.Swain,[18] Z.Szillasi,[42,¶] T.Sztaricskai,[42,¶] X.W.Tang,[7] L.Tauscher,[5] L.Taylor,[11] C.Timmermans,[30] Samuel C.C.Ting,[14] S.M.Ting,[14] S.C.Tonwar,[10] J.Tóth,[13] C.Tully,[34] K.L.Tung,[7]Y.Uchida,[14] J.Ulbricht,[47] E.Valente,[35] G.Vesztergombi,[13] I.Vetlitsky,[27] D.Vicinanza,[37] G.Viertel,[47] S.Villa,[11] M.Vivargent,[4] S.Vlachos,[5] I.Vodopianov,[36] H.Vogel,[33] H.Vogt,[46] I.Vorobiev,[27] A.A.Vorobyov,[36] A.Vorvolakos,[29] M.Wadhwa,[5] W.Wallraff,[1] M.Wang,[14] X.L.Wang,[20] Z.M.Wang,[20] A.Weber,[1] M.Weber,[1] P.Wienemann,[1] H.Wilkens,[30] S.X.Wu,[14] S.Wynhoff,[1] L.Xia,[31] Z.Z.Xu,[20] B.Z.Yang,[20] C.G.Yang,[7] H.J.Yang,[7] M.Yang,[7] J.B.Ye,[20] S.C.Yeh,[50] An.Zalite,[36] Yu.Zalite,[36] Z.P.Zhang,[20] G.Y.Zhu,[7] R.Y.Zhu,[31] A.Zichichi,[9,17,18] F.Ziegler,[46] G.Zilizi,[42,¶] M.Zöller.[1]

1 I. Physikalisches Institut, RWTH, D-52056 Aachen, FRG[§]
III. Physikalisches Institut, RWTH, D-52056 Aachen, FRG[§]
2 National Institute for High Energy Physics, NIKHEF, and University of Amsterdam, NL-1009 DB Amsterdam, The Netherlands
3 University of Michigan, Ann Arbor, MI 48109, USA
4 Laboratoire d'Annecy-le-Vieux de Physique des Particules, LAPP,IN2P3-CNRS, BP 110, F-74941 Annecy-le-Vieux CEDEX, France
5 Institute of Physics, University of Basel, CH-4056 Basel, Switzerland
6 Louisiana State University, Baton Rouge, LA 70803, USA
7 Institute of High Energy Physics, IHEP, 100039 Beijing, China[△]
8 Humboldt University, D-10099 Berlin, FRG[§]
9 University of Bologna and INFN-Sezione di Bologna, I-40126 Bologna, Italy
10 Tata Institute of Fundamental Research, Bombay 400 005, India
11 Northeastern University, Boston, MA 02115, USA
12 Institute of Atomic Physics and University of Bucharest, R-76900 Bucharest, Romania
13 Central Research Institute for Physics of the Hungarian Academy of Sciences, H-1525 Budapest 114, Hungary[‡]
14 Massachusetts Institute of Technology, Cambridge, MA 02139, USA
15 KLTE-ATOMKI, H-4010 Debrecen, Hungary[¶]
16 INFN Sezione di Firenze and University of Florence, I-50125 Florence, Italy
17 European Laboratory for Particle Physics, CERN, CH-1211 Geneva 23, Switzerland
18 World Laboratory, FBLJA Project, CH-1211 Geneva 23, Switzerland
19 University of Geneva, CH-1211 Geneva 4, Switzerland
20 Chinese University of Science and Technology, USTC, Hefei, Anhui 230 029, China[△]
21 SEFT, Research Institute for High Energy Physics, P.O. Box 9, SF-00014 Helsinki, Finland
22 University of Lausanne, CH-1015 Lausanne, Switzerland
23 INFN-Sezione di Lecce and Universitá Degli Studi di Lecce, I-73100 Lecce, Italy
24 Institut de Physique Nucléaire de Lyon, IN2P3-CNRS,Université Claude Bernard, F-69622 Villeurbanne, France
25 Centro de Investigaciones Energéticas, Medioambientales y Tecnologícas, CIEMAT, E-28040 Madrid, Spain♭
26 INFN-Sezione di Milano, I-20133 Milan, Italy
27 Institute of Theoretical and Experimental Physics, ITEP, Moscow, Russia
28 INFN-Sezione di Napoli and University of Naples, I-80125 Naples, Italy
29 Department of Natural Sciences, University of Cyprus, Nicosia, Cyprus
30 University of Nijmegen and NIKHEF, NL-6525 ED Nijmegen, The Netherlands
31 California Institute of Technology, Pasadena, CA 91125, USA
32 INFN-Sezione di Perugia and Universitá Degli Studi di Perugia, I-06100 Perugia, Italy
33 Carnegie Mellon University, Pittsburgh, PA 15213, USA
34 Princeton University, Princeton, NJ 08544, USA
35 INFN-Sezione di Roma and University of Rome, "La Sapienza", I-00185 Rome, Italy
36 Nuclear Physics Institute, St. Petersburg, Russia
37 University and INFN, Salerno, I-84100 Salerno, Italy
38 University of California, San Diego, CA 92093, USA
39 Dept. de Fisica de Particulas Elementales, Univ. de Santiago, E-15706 Santiago de Compostela, Spain
40 Bulgarian Academy of Sciences, Central Lab. of Mechatronics and Instrumentation, BU-1113 Sofia, Bulgaria
41 Center for High Energy Physics, Adv. Inst. of Sciences and Technology, 305-701 Taejon, Republic of Korea
42 University of Alabama, Tuscaloosa, AL 35486, USA
43 Utrecht University and NIKHEF, NL-3584 CB Utrecht, The Netherlands
44 Purdue University, West Lafayette, IN 47907, USA
45 Paul Scherrer Institut, PSI, CH-5232 Villigen, Switzerland
46 DESY, D-15738 Zeuthen, FRG
47 Eidgenössische Technische Hochschule, ETH Zürich, CH-8093 Zürich, Switzerland
48 University of Hamburg, D-22761 Hamburg, FRG
49 National Central University, Chung-Li, Taiwan, China
50 Department of Physics, National Tsing Hua University, Taiwan, China

§ Supported by the German Bundesministerium für Bildung, Wissenschaft, Forschung und Technologie
‡ Supported by the Hungarian OTKA fund under contract numbers T019181, F023259 and T024011.
¶ Also supported by the Hungarian OTKA fund under contract numbers T22238 and T026178.
♭ Supported also by the Comisión Interministerial de Ciencia y Tecnología.
♯ Also supported by CONICET and Universidad Nacional de La Plata, CC 67, 1900 La Plata, Argentina.
♢ Also supported by Panjab University, Chandigarh-160014, India.
△ Supported by the National Natural Science Foundation of China.

† Deceased.

Decay Channel	BRANCHING RATIOS $M = 90$ GeV $f = f'$	$M = 90$ GeV $f = -f'$	$M = 180$ GeV $f = f'$	$M = 180$ GeV $f = -f'$
$\ell^* \to \ell\gamma$	89%	0%	37%	0%
$\ell^* \to \nu\mathrm{W}$	11%	99%	54%	63%
$\ell^* \to \ell\mathrm{Z}$	0%	1%	9%	37%
$\nu^* \to \nu\gamma$	0%	89%	0%	37%
$\nu^* \to \ell\mathrm{W}$	99%	11%	63%	54%
$\nu^* \to \nu\mathrm{Z}$	1%	0%	37%	9%

Table 1: Predicted branching ratios for charged and neutral excited lepton decays, for different choices of masses and couplings.

<table>
<tr><th rowspan="2"></th><th colspan="4">Radiative Decays</th><th colspan="4">Weak Decays</th></tr>
<tr><th>Signal</th><th>N_D</th><th>N_B</th><th>ϵ</th><th>Signal</th><th>N_D</th><th>N_B</th><th>ϵ</th></tr>
<tr><td rowspan="6">Pair Production</td><td>$\mathrm{e}^*\mathrm{e}^* \to \mathrm{ee}\gamma\gamma$</td><td>0</td><td>0.6</td><td>49%</td><td rowspan="3">$\ell^*\ell^* \to \nu\nu\mathrm{WW}$</td><td rowspan="4">2710</td><td rowspan="4">2765</td><td rowspan="3">67%</td></tr>
<tr><td>$\mu^*\mu^* \to \mu\mu\gamma\gamma$</td><td>0</td><td>0.4</td><td>46%</td></tr>
<tr><td>$\tau^*\tau^* \to \tau\tau\gamma\gamma$</td><td>1</td><td>0.2</td><td>40%</td></tr>
<tr><td rowspan="3">$\nu^*\nu^* \to \nu\nu\gamma\gamma$</td><td rowspan="3">2</td><td rowspan="3">1.6</td><td rowspan="3">44%</td><td>$\nu_\tau^*\nu_\tau^* \to \tau\tau\mathrm{WW}$</td><td>71%</td></tr>
<tr><td>$\nu_\mathrm{e}^*\nu_\mathrm{e}^* \to \mathrm{eeWW}$</td><td>1</td><td>0.12</td><td>18%</td></tr>
<tr><td>$\nu_\mu^*\nu_\mu^* \to \mu\mu\mathrm{WW}$</td><td>1</td><td>0.34</td><td>21%</td></tr>
<tr><td rowspan="6">Single Production</td><td>$\mathrm{e}^*\mathrm{e} \to \mathrm{ee}\gamma$</td><td>563</td><td>564</td><td>63%</td><td>$\mathrm{e}^*\mathrm{e} \to \nu_\mathrm{e}\mathrm{We}$</td><td>452</td><td>455</td><td>24%</td></tr>
<tr><td>$\mu^*\mu \to \mu\mu\gamma$</td><td>71</td><td>64</td><td>61%</td><td>$\mu^*\mu \to \nu_\mu\mathrm{W}\mu$</td><td>476</td><td>479</td><td>49%</td></tr>
<tr><td>$\tau^*\tau \to \tau\tau\gamma$</td><td>64</td><td>55</td><td>43%</td><td>$\tau^*\tau \to \nu_\tau\mathrm{W}\tau$</td><td>1004</td><td>972</td><td>44%</td></tr>
<tr><td rowspan="3">$\nu^*\nu \to \nu\nu\gamma$</td><td rowspan="3">191</td><td rowspan="3">219</td><td rowspan="3">66%</td><td>$\nu_\mathrm{e}^*\nu_\mathrm{e} \to \mathrm{eW}\nu_\mathrm{e}$</td><td>452</td><td>455</td><td>47%</td></tr>
<tr><td>$\nu_\mu^*\nu_\mu \to \mu\mathrm{W}\nu_\mu$</td><td>476</td><td>479</td><td>51%</td></tr>
<tr><td>$\nu_\tau^*\nu_\tau \to \tau\mathrm{W}\nu_\tau$</td><td>1004</td><td>972</td><td>41%</td></tr>
</table>

Table 2: Number of candidates N_D, number of background events N_B, and average signal efficiencies ϵ, for radiative and weak decays, in the pair production (upper part) and the single production (lower part) searches.

Excited Lepton	95% CL Mass Limit (GeV)		
	$f = f'$	$f = -f'$	Coupling Independent
e^*	94.2	92.6	92.4
μ^*	94.2	92.6	92.4
τ^*	94.2	92.6	91.7
ν_e^*	93.9	94.1	93.4
ν_μ^*	94.0	94.1	93.5
ν_τ^*	91.5	94.1	90.2

Table 3: 95% confidence level lower mass limits for the different excited leptons obtained from pair production searches. For each flavour, the mass limits for $f = f'$, $f = -f'$ and for the coupling independent case, are shown.

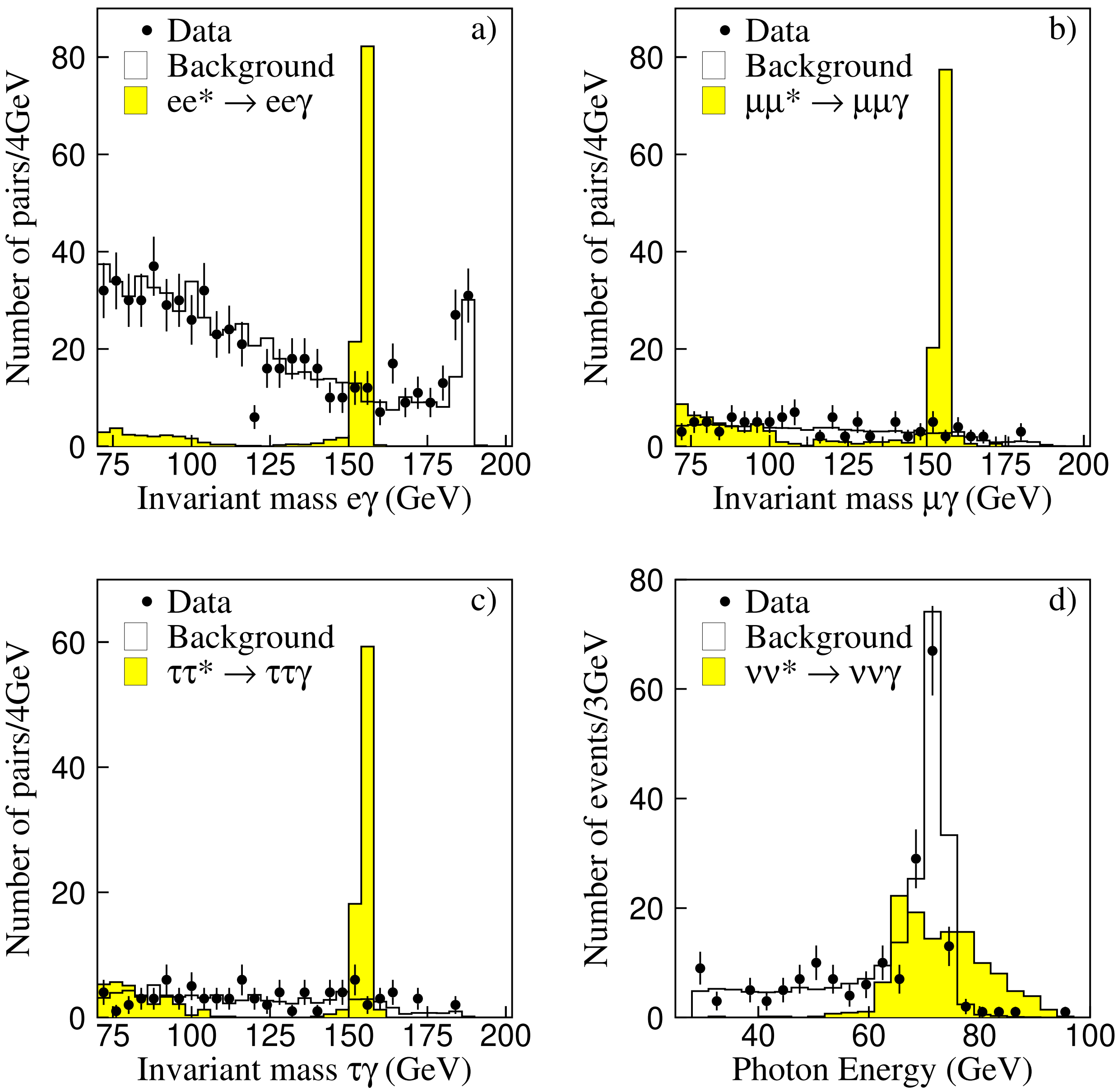

Figure 1: The invariant mass distributions for (a) $e\gamma$, (b) $\mu\gamma$, and (c) $\tau\gamma$ pairs. Energy distribution of single photon events (d). The expected signal for an excited lepton with a mass of 155 GeV normalised to 1.0 pb for all the channels is shown together with data and Standard Model background.

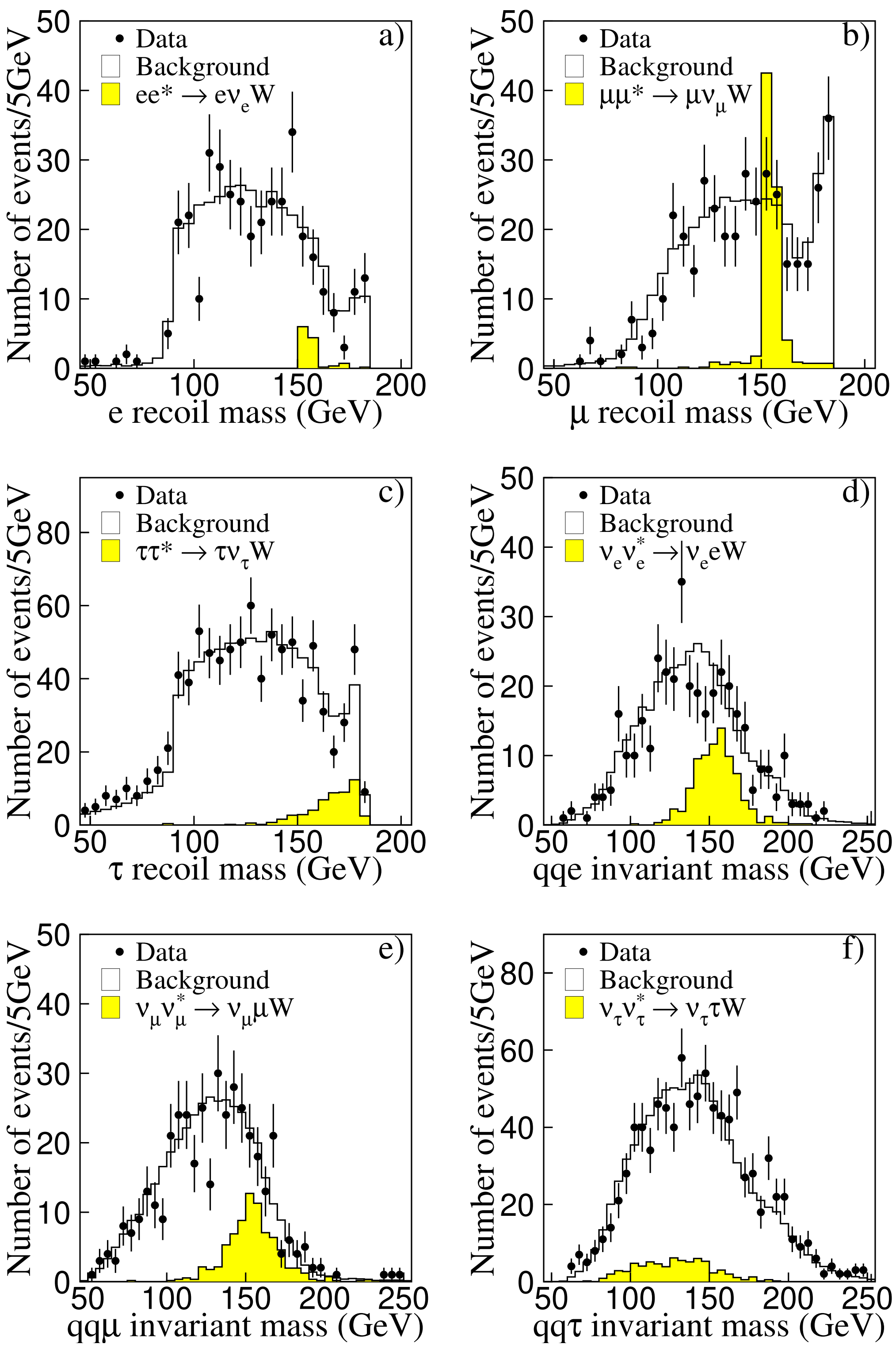

Figure 2: Recoil mass distributions for (a) electron , (b) muon , and (c) tau, in the qqℓ selections. Invariant mass distributions for (d) qqe, (e) qqμ, and (f) qqτ, selected events. The expected signal for an excited lepton with a mass of 155 GeV normalised to 1.0 pb for all the channels is shown together with data and Standard Model background.

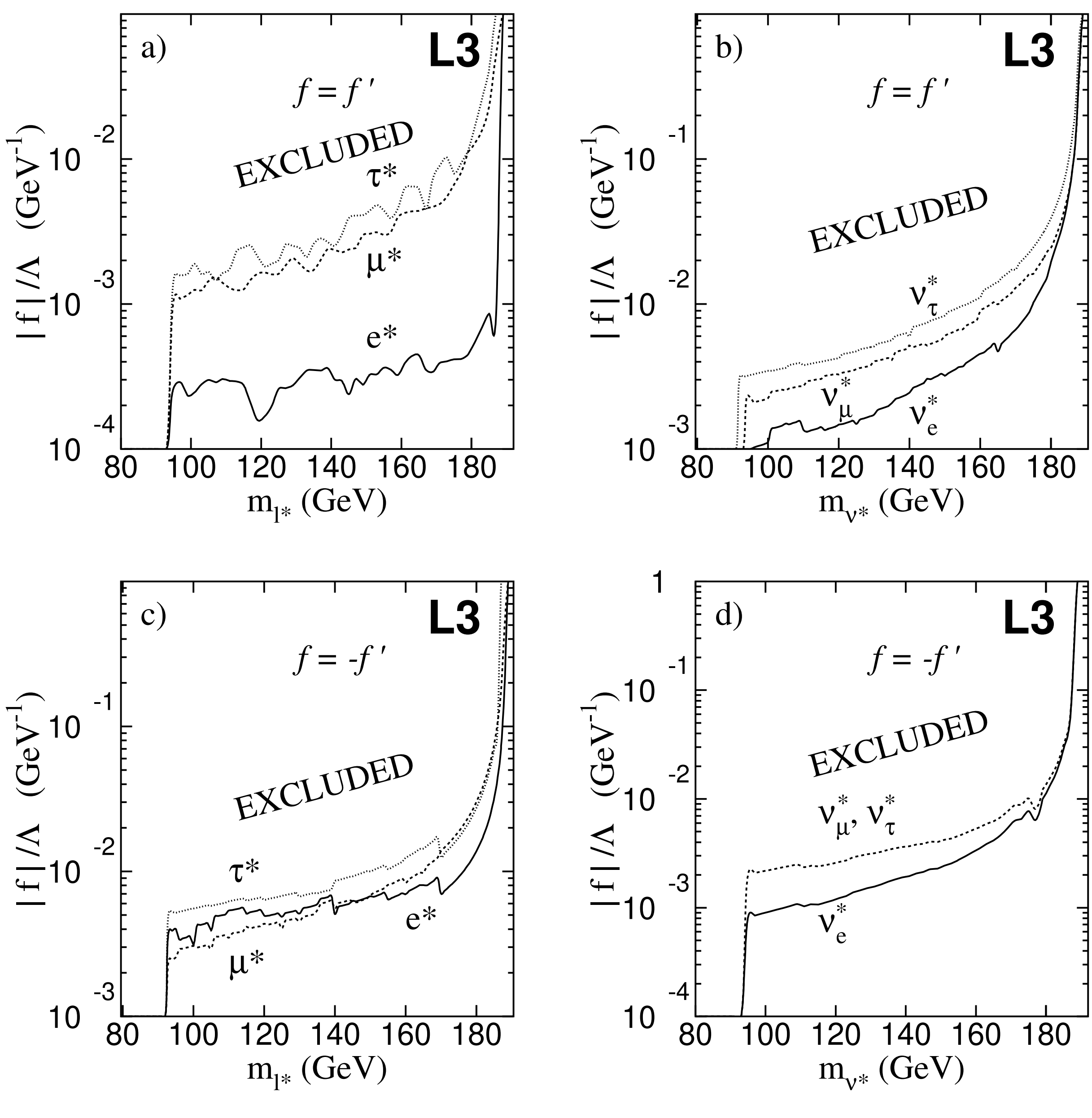

Figure 3: 95% confidence level upper limit on the coupling constant $|f|/\Lambda$, as a function of the excited lepton mass with $f = f'$: (a) e^*, μ^* and τ^* , (b) ν_e^*, ν_μ^* and ν_τ^*, and with $f = -f'$: (c) e^*, μ^* and τ^*, (d) ν_e^*, ν_μ^* and ν_τ^*.